https://doi.org/10.5194/egusphere-2025-1407
Preprint. Discussion started: 15 May 2025

Optimizing Ammonia Emissions for $PM_{2.5}$ Mitigation: Environmental and Health Co-Benefits in Eastern China

Keqin Tang [1], Haoran Zhang [2], Ge Xu [1], Fengyi Chang [1], Yang Xu [1], Ji Miao [3], Xian Cui [4], Jianbin Jin [1], Baojie Li [1], Ke Li [1], Hong Liao [1], Nan Li [1,*]

[1] Jiangsu Key Laboratory of Atmospheric Environment Monitoring and Pollution Control, Jiangsu Collaborative Innovation Center of Atmospheric Environment and Equipment Technology, School of Environmental Science and Engineering, Nanjing University of Information Science & Technology, Nanjing, 210044, China

[2] School of Atmospheric Sciences, Nanjing University, Nanjing, China

[3] Department of Colorectal Surgery, Nanjing Drum Tower Hospital, Affiliated Hospital of Medical School, Nanjing University, Nanjing, China

[4] Rugao Hospital of Chinese Medicine, Nantong, China

[*] *Correspondence to: Nan Li, linan@nuist.edu.cn*

https://doi.org/10.5194/egusphere-2025-1407
Preprint. Discussion started: 15 May 2025

Abstract.

Ammonia (NH_3) is a key precursor of $PM_{2.5}$, contributing to the formation of secondary inorganic aerosols and playing a crucial role in haze events. However, current bottom-up emission inventories in China often underestimate NH_3 emissions, particularly with significant uncertainties in urban areas. This study developed a "top-down" iterative algorithm that integrates the IASI satellite observations with the WRF-Chem model to optimize bottom-up NH_3 emissions, and further quantified the impacts of source-specific emission reductions on $PM_{2.5}$ pollution. The result reveals that the updated NH_3 emissions in Eastern China for 2016 amounted to 4.2 $Tg \cdot yr^{-1}$, 27.3% higher than prior estimations. The optimized NH_3 emissions peak in summer at 463.1 $Gg \cdot mon^{-1}$, with agricultural sources accounting for 85%, while winter emissions drop to 217 $Gg \cdot mon^{-1}$ when the contribution from non-agricultural sources (e.g., industry, vehicle) significantly increases. The optimized NH_3 emission significantly improved the simulated results of NH_3 concentration, both in terms of magnitude (31%~42%) and variations (17%~55%). Sensitivity simulations show that a 30%~60% reduction in NH_3 emission led to decreases of 1.5~8.8 $\mu g \cdot m^{-3}$ in city-level $PM_{2.5}$ concentrations and the potential effect of reducing non-agricultural emissions is comparable with that from agricultural sources. Furthermore, the NH_3 reduction positively impacts public health, resulting in a 6.5%~10.3% decrease in premature deaths attributed to $PM_{2.5}$ exposure. These findings provide strong data support for air quality research and offer valuable insights into the potential air quality and public health benefits of NH_3 emission reduction.

Keywords: NH_3 emission, $PM_{2.5}$, satellite retrieval, WRF-Chem, top-down

https://doi.org/10.5194/egusphere-2025-1407
Preprint. Discussion started: 15 May 2025

1 Introduction

In recent years, China has continued to face significant challenges associated with $PM_{2.5}$ pollution (Geng et al., 2024; Lei et al., 2022). This issue adversely affects atmospheric environment via reducing visibility (Hu et al., 2021; Yang et al., 2022) and deteriorating air quality (Lei et al., 2024; Song et al., 2025), impacts climate change by altering radiation balance and cloud formation (Gao et al., 2023; Yang et al., 2021), and poses substantial threats to human health (Du et al., 2024; Feng et al., 2016; Liu et al., 2025; Xiao et al., 2022; Zhu et al., 2025). Ammonia (NH_3), a key precursor of $PM_{2.5}$, neutralizes sulfuric acid (H_2SO_4) and nitric acid (HNO_3), leading to the formation of secondary inorganic aerosols (SIA), which contributes 19.4%~55。0% of the total $PM_{2.5}$ (Huang et al., 2014; Liu et al., 2022b; Wang et al., 2016; Wei et al., 2023; Zheng et al., 2015; Zhou et al., 2022). Reducing NH_3 emissions is a highly effective strategy for mitigating of $PM_{2.5}$ pollution (Bessagnet et al., 2014; Xu et al., 2022), particularly in light of the successful control of sulfur dioxide (SO_2) and nitrogen dioxide (NO_2) in China over the past decade (Li et al., 2023b; Wang et al., 2017; Zhang et al., 2019; Zheng et al., 2018).

The anthropogenic sources of NH_3 include agriculture, industry, power generation, transportation and residential activities. Numerous studies have estimated NH_3 emissions using a bottom-up approach, reporting emissions in China ranging from 9.7 Tg yr^{-1} to 13.2 Tg yr^{-1} (Chen et al., 2021; Huang et al., 2012; Kang et al., 2016; Li et al., 2021; Ma, 2020). Among these sources, agricultural (AGR) sector is identified as the dominant contributor nationwide, accounting for 75.0%~94.5% of total NH_3 emissions (Guo et al., 2020; Ma, 2020; Zhou et al., 2021). Additionally, some studies have highlighted that in densely populated regions, NH_3 from non-agricultural (non-AGR) activities, such as industrial production/slip, vehicles, and waste disposal, contributing up to 50% of regional emissions and should not be overlooked, (Chang et al., 2015, 2016; Chen et al., 2022; Feng et al., 2022; Pan et al., 2016, 2018b; Pu et al., 2020; Song et al., 2021; Sun et al., 2017; Van Damme et al., 2018; Wu et al., 2020). However, despite considerable progress, bottom-up estimates still exhibit considerable

https://doi.org/10.5194/egusphere-2025-1407
Preprint. Discussion started: 15 May 2025

discrepancies and are often outdated, with a time lag of 1~2 years, mainly due to the lack of accurate and timely statistical data.

The uncertainty in the emission estimations further contributes to significant discrepancies (1%~50%) in the assessing impacts of NH_3 reduction on $PM_{2.5}$ level (Guo et al., 2018, 2024; Li et al., 2024; Liu et al., 2019, 2021, 2023; Pan et al., 2024; Zhang et al., 2022). Cheng et al (2021) employed WRF-Chem simulations to demonstrate a 24.6% reduction in $PM_{2.5}$ from the removal of AGR NH_3 emissions. Concurrently, Ti et al (2022) determined that a 74% decrease in AGR NH_3 resulted in a 34.9% reduction in $PM_{2.5}$ in China.

To enhance the accuracy and reliability of bottom-up emission estimations, air quality monitoring satellites are increasingly regarded as valuable tools from a top-down perspective, offering advantages in both magnitude and timeliness (Chen et al., 2021; Guo et al., 2020; Jin et al., 2023; Qi et al., 2017; Zhou et al., 2021, 2017) . Many studies have estimated optimized NH_3 emissions in China to be between 10.0 Tg yr^{-1} and 18.9 Tg yr^{-1} by coupling chemical transport model, mass balance approach, or machine learning techniques with various NH_3 measurements (satellite retrieval or ground monitoring). Some studies have also improved the description of the spatial and monthly variations of NH_3 emissions (Kong et al., 2019; Liu et al., 2022a; Paulot et al., 2014; Zhang et al., 2018, 2017). However, most top-down studies lack further investigation into the source-specific allocation of emissions based on the optimal total emission assessment (Fu et al., 2015; Sun et al., 2017; Zhang et al., 2024). Hence, a more comprehensive understanding of NH_3 emissions from diverse sources across varying seasons is needed to improve existing top-down inventories and enhance the scientific accuracy of NH_3 emission reduction assessments.

In this study, we used satellite and surface NH_3 measurements alongside the regional chemical model WRF-Chem to constrain bottom-up and source-specific NH_3 emission estimates over Eastern China, with the aim of more accurately assessing the impacts of NH_3 emission reductions from different sources on $PM_{2.5}$ concentrations. The paper is structured as follows: Section 2 describes the detailed methodology, Section 3 presents the simulated NH_3 with prior emission, Section 4 provides a top-

https://doi.org/10.5194/egusphere-2025-1407
Preprint. Discussion started: 15 May 2025

down estimate of NH_3 emission, and Section 5 demonstrates the direct correlation between NH_3 emission reductions and $PM_{2.5}$ concentration levels, as well as the resulting health benefits. Our work differs from previous studies in that we constrain NH_3 emissions by sector, season, and region, and further assess the potential mitigation effects of NH_3 based on the optimized NH_3 inventory.

2 Methodology

2.1 Air Quality Model

In this study, the chemical transport model WRF-Chem v3.9.1 (Grell et al. 2005) was utilized to constrain the NH_3 emissions and to assess the impact of reduced NH_3 emission on $PM_{2.5}$ concentrations. Spatially, two nested domains were configured with horizontal resolutions of 54×54 km^2 and 18×18 km^2. The outer domain covered entire China and the inner domain focused Eastern China, characterized by intensive anthropogenic activities and elevated pollution levels(Pendergrass et al., 2025; Peng et al., 2025), including the Beijing-Tianjin-Hebei (BTH) region, Henan, Shandong, and the Yangtze River Delta (YRD) region (Figure 1). The initial and boundary conditions of meteorological parameters were derived from FNL reanalysis datasets provided by the National Centers for Environmental Prediction (NCEP) in the United States (https://rda.ucar.edu/datasets/). The initial and boundary conditions of chemical species were obtained from the global chemical model MOZART (Emmons et al. 2010). We conducted simulations for the entire year of 2016. The physical and chemical parameterization for describing sub-grid processes, such as radiation, microphysics, and gas-phase reaction schemes, are listed in Table S1.

We adopted anthropogenic emission estimates from the Multi-resolution Emission Inventory for China (MEIC) developed by Tsinghua University (Li et al., 2017; Zheng et al., 2018). Moreover, biogenic emissions and biomass burning emissions were calculated online using the Model of Emissions of Gases and Aerosols from Nature (MEGAN, v2.0.4) (Guenther, 2006) and the Fire Inventory from NCAR (FINN) (Wiedinmyer et al., 2011), respectively.

https://doi.org/10.5194/egusphere-2025-1407
Preprint. Discussion started: 15 May 2025

2.2 Satellite retrievals and surface measurements

We obtained the total NH_3 column density data from the IASI dataset (https://iasi.aeris-data.fr/nh3/, last accessed on May 13, 2025) to represent the observed NH_3 level. The inversion algorithm used in IASI is the ANNI-NH_3 algorithm, which is based on the HRI inversion framework developed by Damme et al (2017) without averaging kernels. The IASI NH_3 products feature daily temporal resolution and fine spatial resolution (12×12 km^2). In this study, we pre-processed the data of IASI products into monthly averages to achieve high spatial coverage and interpolated them to the grid cells of the WRF-Chem model. Furthermore, an artificial neural network is employed to enhance the accuracy and confidence of the IASI product. We selected the products with less than 75% uncertainty and less than 10% cloud coverage.

In addition, surface NH_3 observation from in-situ measurements reported by Pan et al. (2018a) were employed for simulation evaluation. These ground-based measurements summarized the seasonal mean concentration of NH_3 at 53 sites in China from September 2015 to August 2016.

Additionally, surface meteorological data, including temperature, relative humidity and wind speed was obtained from China Meteorological Administration website (https://data.cma.cn/) to assess the meteorological conditions in study region. Air pollutant concentrations associated with NH_3 (such as $PM_{2.5}$, NO_2 and SO_2) from public website of the Ministry of Ecology and Environment (MEE) (https://air.cnemc.cn:18007/) of China were also used for evaluation. The complete information of the in-situ measurements used in this study is available in Tables S2~S4.

3 NH_3 simulations with bottom-up emissions

We applied the bottom-up NH_3 emission from MEIC (Li et al., 2017; Zheng et al., 2018) to drive the prior simulation. As shown in Figure 2, the prior NH_3 emission amounted to 3.3 Tg yr^{-1} in Eastern China, among which 93.0% emission is from AGR sources and the other 7.0% emission is from non-AGR sources. The largest emissions

https://doi.org/10.5194/egusphere-2025-1407
Preprint. Discussion started: 15 May 2025

are recorded in July at 366.8 Gg mon $^{-1}$, while the smallest emissions are recorded in January at 206.5 Gg mon $^{-1}$ (Figure S1).

We compared the model results from prior run (for the entire year of 2016) with the satellite retrievals and the in-situ NH_3 measurements. To quantitatively describe model performance, we adopted three following statistical metrics, i.e., root mean squared error (RMSE, 0 ~ +∞), index of agreement (IOA, 0 ~ 1) and mean fractional bias (MFB, -2 ~ 2)(Huang et al., 2021). They were calculated based on Eq. 1~3, where subscripts s, o and N represent simulation, observation, and the number of samples, respectively.

$$RMSE = \sqrt{\frac{\sum_{i=1}^{N}(C_m - C_o)^2}{N}} \quad (1)$$

$$IOA = 1 - \frac{\sum_{i=1}^{N}(C_s - C_o)^2}{\sum_{i=1}^{N}(|C_s - \overline{C_o}| + |C_o - \overline{C_o}|)^2} \quad (2)$$

$$MFB = \frac{1}{N}\sum_{i=1}^{N}\frac{(C_o - C_m)}{(\frac{C_o + C_m}{2})} \quad (3)$$

The annual NH_3 total column density is simulated to be 17.4×10^{15} molec cm^{-2} averaged for Eastern China, which represents a 61% underestimated compared to satellite retrievals (29.0×10^{15} molec cm^{-2}). The seasonal simulations of NH_3 results also exhibit significant discrepancies with observations, especially in the spring. Specifically, the simulated NH_3 total column in Eastern China is only 13.2×10^{15} molec cm^{-2} in spring, with concentration in 67.5% of the region being underestimated by more than 50%. These discrepancies are also evident in Figure 3. Most simulated NH_3 total columns have errors of over 30% when compared to satellite columns, and the RMSE of 10.

Spatially, satellite-based observations reveal that the high-value areas of NH_3 column are located at the junction of Henan, Shandong, and Hebei provinces. In contrast, the prior modeling results show that NH_3 column densities are more concentrated in Henan. This indicates a clear discrepancy in the spatial distribution of NH_3 column density between the prior simulations and the observations.

Additionally, the comparison between the simulated and observed surface NH_3 concentrations also indicates a notable underestimation. The mean simulated surface NH_3 concentration over the study region is 6.3 μg m^{-3}, which is only half of the

https://doi.org/10.5194/egusphere-2025-1407
Preprint. Discussion started: 15 May 2025

observation value, with an IOA of 0.56 and an MFB of -61% (Figure S2).

4 Top-down estimates of NH_3 emissions

4.1 Iterative algorithm for NH_3 emission estimation

We utilized an iterative algorithm (Figure 4) to update the prior NH_3 emissions from different sources constrained by IASI observations. This process was carried out in January, April, July, and October in 2016 to represent four seasons. We compared the prior simulation results with satellite retrievals and discussed the performance of prior emissions in detail in Section 3. Furthermore, we conducted a series of sensitivity simulations to obtain prior simulated NH_3 from disparate sources and which were then fed into the iterative algorithm along with satellite data for calculation. In each iterative calculation, the monthly average satellite-derived NH_3 column concentration in single-pixel served as the target, and multiple linear regression (MLR) was applied to calculate the corresponding regression factors for AGR and non-AGR emissions (Figure S3). Here, we take the *i* iteration in *k* month, *j* region as an example to calculate the regression factors, and the formula is as follows:

$$\mathrm{TA_{satellite}}^{j,k} - \mathrm{SA_{transport}}^{j,k} = \alpha_i^{j,k} * \mathrm{SA_{agriculture}}_{i-1}^{j,k} + \beta_i^{j,k} * \mathrm{SA_{non-agriculture}}_{i-1}^{j,k} \quad (4)$$

where, $\mathrm{TA_{satellite}}^{j,k}$ denotes the total NH_3 column density retrieved from the IASI satellite data, and $\mathrm{SA_{transport}}^{j,k}$, $\mathrm{SA_{agriculture}}_{i-1}^{j,k}$ and $\mathrm{SA_{non-agriculture}}_{i-1}^{j,k}$ stand for the total column concentration of NH_3 contributed by AGR emissions, non-AGR emissions, and outside transportation, respectively. We clarified this NH_3 concentrations contributed by different pathways by conducting sensitivity tests with the WRF-Chem model (Table 2). In each cycle, we control AGR emissions, non-AGR emissions and regional external emissions to obtain the corresponding NH_3 column concentration. The $\mathrm{SA_{agriculture}}_{i-1}^{j,k}$, $\mathrm{SA_{non-agriculture}}_{i-1}^{j,k}$, and $\mathrm{SA_{transport}}^{j,k}$ are calculated by subtracting A_{blank} from A_{agr}, $A_{non-agr}$, and $A_{transport}$, respectively.

Further, the multiple linear regression provided regression coefficients $\alpha_i^{j,k}$ and $\beta_i^{j,k}$, respectively correspond to AGR and non-AGR NH_3 emissions in month *j* from area

https://doi.org/10.5194/egusphere-2025-1407
Preprint. Discussion started: 15 May 2025

k, within the *i* iteration. As the regression equation is obtained in a mathematical statistical sense, we need to correct for this regression coefficient. The biases between the model simulation and the satellite retrievals were calculated as $D_i^{j,k}$. We considered the residuals of the multiple linear regression, the goodness of fit and $D_i^{j,k}$, and obtained the judgment coefficient $K_i^{j,k}$. The regression coefficients with excessive residuals are removed to increase credibility. Concurrently, the goodness of fit of the regression is calculated. In the event that the goodness of fit falls between 0.3 and 1, the regression coefficient is deemed to be acceptable. Should the regression coefficient fail to meet the requisite requirements, it is deemed invalid. We further use it to make a trade-off for the regression coefficient. The adjustment factors a and b for AGR and non-AGR sources were finally obtained, respectively. Finally, the new simulated NH_3 values were obtained through WRF-Chem, and the process was iteratively repeated, until the error is less than 30%. It is worth noting that we conducted detailed temporal (month) and spatial divisions (grid) in the MLR analysis and calculated them separately to better capture the seasonal and spatial characteristics of emissions.

4.2 posterior NH_3 emission estimates

The top-down constrained results (posterior) indicate that the annual NH_3 emission in Eastern China has been updated to 4.2 Tg yr^{-1}, representing a 27.3% increase compared to the prior value (Figure 2). The posterior non-AGR emissions show a significant increase, from 0.2 Tg yr^{-1} to 1.1 Tg yr^{-1}, particularly in urban regions along the Yangtze River, as well as in southern BTH, central Shandong and northern Henan. The posterior AGR emissions increased slightly, from 3.0 Tg yr^{-1} to 3.1 Tg yr^{-1}, but the high-emission regions shift from Henan to Shandong, Jiangsu and northern Anhui (Ren et al., 2023).

In terms of seasonality, as shown in Figure 5, the posterior NH_3 emissions are highest in summer, with a total of 463.1 Gg mon^{-1}, followed by spring (442.4 Gg mon-

https://doi.org/10.5194/egusphere-2025-1407
Preprint. Discussion started: 15 May 2025

^{1}), largely due to fertilizer application (Li et al., 2021; Lu et al., 2025; Ren et al., 2025), and lowest in winter (217.4 Gg mon^{-1}). At the specific-source scale, AGR NH_3 emissions show similar seasonal patterns with the total NH_3 emissions, higher in summer and spring. In contrast, non-AGR NH_3 are highest in winter and fall because fossil fuel combustion-related emissions are high in cold season, while the lowest emissions occur in summer. In addition, the ratio of AGR and non-AGR NH_3 emissions significantly varies across different regions. The percentages of non-AGR NH_3 emissions range from 18.8% to 35.8%, which is higher than the proportion in the prior inventory (Figure 5a). This shift can be attributed to the increased relative importance of fossil fuel combustion-related emissions under high $PM_{2.5}$ loadings, which in turn promote higher NH_3 emissions from these sources (Pan et al., 2018b). Meanwhile, AGR NH_3 emissions are relatively inactive in winter due to unfavorable meteorological conditions. Similar high fractions of non-AGR emissions have also been reported in other studies (Feng et al., 2022; He et al., 2021).

Table 1 compares the results with related studies focused on NH_3 emission estimates. Overall, the estimated NH_3 emission in this study is comparable to the estimates of the other studies based on "top-down" and "bottom-up" approaches. In similar years and regions, the discrepancy between the estimates of this study and other studies ranges from 1.0% to 19.6%. Furthermore, the seasonal distribution of NH_3 emissions in this study aligns with the findings of some prior research (Kong et al., 2019; Liu et al., 2024; Zhang et al., 2018; Zhao et al., 2020). In terms of sectors, other studies have indicated that the proportion of NH_3 emissions from AGR sources is more than 80%, using the bottom-up approach (Chen et al., 2021; Huang et al., 2012; Kang et al., 2016; Li et al., 2021). This study, however, reveals a proportion of 74.4% for AGR emissions, thereby emphasizing the contribution of non-AGR emissions. By employing an iterative algorithm for the estimation of NH_3 emissions from diverse sources, this study facilitates a more comprehensive capture of neglected non-AGR sources. Concurrently, the eastern developed industry is expected to exhibit an increase in the proportion of NH_3 emissions from non-AGR sources when compared to the national average. It is important to note that discrepancies in results between studies

https://doi.org/10.5194/egusphere-2025-1407
Preprint. Discussion started: 15 May 2025

may be attributable to methodological differences (e.g. the sensitivity of the top-down approach to target data selection) and uncertainty in the underlying data. For instance, the NH_3 emission estimated by Paulot et al. (2014) using the mass balance method based on NH_4^+ wet deposition fluxes is significantly lower than that in other studies, which may be attributed to its fewer observation sites in China. These discrepancies underscore the necessity to enhance the reliability of NH_3 observations in forthcoming studies, with the objective of enhancing the precision of the estimates.

4.3 Simulated NH_3 with top-down emissions

Figure 6 compares the spatial distributions of NH_3 total column density from satellite retrievals, prior simulations and posterior simulations. The annual mean simulated NH_3 total column density from posterior emissions is 23.7×10^{15} molec cm^{-2}, 35.9% higher than the prior results and closer to the observed 29.0×10^{15} molec cm^{-2}. IOA and MFB between the posterior simulations versus measurements are 0.9 and -30.0%. Figure 3 also shows the improvement in model performance. More than 80% of the points fall in the range where the simulation-to-observation ratio is between 0.7 and 1.3 and the RMSE is less than 10. A more consistent seasonal distribution can be obtained in a posterior simulation, with associated temporal MFB of NH_3 column density on the seasonal scale is reduced from -53% (prior) to -24% (posterior). Simultaneously, the spatial distribution pattern of posterior simulation is more identical to the characteristics revealed by satellite-based observations (Figure 6). The spatial MFB is also decreased from -52% (prior) to -20% (posterior), with an increase in spatial correlation coefficient from 0.79 to 0.92. The improvement is especially notable in the BTH region, where the simulated NH_3 column densities are doubled.

A similar improvement is also witnessed in the modeling of the surface NH_3 concentrations. The utilization of posterior emissions effectively reduces the bias of annual average NH_3 surface concentration by 42%. The MFBs of surface NH_3 simulation of seasons decrease from -79.0%~-37.0% to –47.0%~12.0% and the IOAs increase from 0.49~0.67 to 0.56~0.72. As illustrated in Figure S2, the posterior simulations successfully capture the spatial and seasonal characteristics against the surface measurements. Nevertheless, the mean annual simulated surface NH_3 concentration still exhibits an underestimation (MFB = -19.0%). The obvious underestimation can be found in Yuncheng and Cangzhou, BTH (Table S2), which is further attributed to the impacts of local land use types categorized as farmlands and suburban (Pan et al., 2018a).

Furthermore, improving the NH_3 simulation results in the other simulated air pollutants being closer to observed levels (Table 3). It was found that posterior NH_3 emissions effectively bridge the gap between simulated and observed $PM_{2.5}$. The average $PM_{2.5}$ concentration increased from 65.7 μg m^{-3} to 67.3 μg m^{-3}, which is closer to the observed value of 67.1 μg m^{-3}. Additionally, posterior SO_2 levels decreased by 17.1% in cities, from 8.2 ppbv to 6.8 ppbv, closer to observed 6.5 ppbv. The successful capture of air pollutants highlights a significant improvement in the NH_3 emission inventory for eastern China. The evaluation of routine air pollutants in each city is detailed in Figures S4~S6. The statistics of evaluation metrics for each city's meteorological simulation can also be found in Table S5.

5 $PM_{2.5}$ and its health burden response to NH_3 reduction

To investigate the response of $PM_{2.5}$ to various NH_3 emission reduction scenarios, we conducted sensitivity tests as outlined in Table S6. We formulated emission reduction scenarios of 30%~60% for January and July of 2016, considering the severe particulate pollution in winter and the higher NH_3 concentrations in summer. Emission reductions from both the AGR and non-AGR sectors were considered separately.

Figure 7 illustrates that reducing NH_3 emissions by 30%~60% can decrease the seasonal $PM_{2.5}$ concentration by 1.5~5.7 μg m^{-3} averaged for Eastern China in winter, mainly due to the reduction in secondary inorganic aerosols (SIA). Specifically, nitrate, ammonium and sulfate are reduced by 0.9~3.3 μg m^{-3}, 0.4~1.3 μg m^{-3} and 0.3~1.0 μg m^{-3} respectively. It is worth noting that the reduction in sulfate is smaller than that in nitrate because NH_3 preferentially reacts with sulfuric acid during aerosol formation (Figure S7). When ambient NH_3 concentrations are limited, nitrate concentrations decrease more significantly than sulfate concentrations. In summer, although aerosol

https://doi.org/10.5194/egusphere-2025-1407
Preprint. Discussion started: 15 May 2025

pollution is relatively lower, NH_3 emissions and atmospheric reactivity are higher. Consequently, reducing emissions by the same percentage results in a decrease in $PM_{2.5}$ concentration by 5.5~8.8 μg m^{-3}.

In terms of special sources, reducing non-AGR NH_3 emissions is just as crucial as reducing AGR NH_3 emissions in mitigating $PM_{2.5}$. A 30% to 60% reduction in non-AGR NH_3 emissions during winter can lead to a decrease in $PM_{2.5}$ by 0.9~1.5 μg m^{-3}, which is comparable to the effect of reducing AGR NH_3 emissions (0.9~2.0 μg m^{-3}). It should be noted that the reduction in $PM_{2.5}$ resulting from both AGR and non-AGR NH_3 emissions is not proportional to the emission reduction across all sectors. This is due to the non-linear relationship between NH_3 emissions and $PM_{2.5}$ concentrations.

This study utilized the integrated exposure–response (IER) model to estimate premature mortality resulting from $PM_{2.5}$ exposure. Detailed methods and data can be found in our previous work (Li et al., 2023a). In the base case, $PM_{2.5}$ exposure exhibits a significant impact on premature mortality, leading to 698.4 thousand fatalities in the study region. Specifically, premature deaths attributable to ischemic heart disease (IHD), stroke, lung cancer (LC), and chronic obstructive pulmonary disease (COPD) are 202.3, 347.9, 61.5, and 86.7 thousand, respectively. In other scenarios, the overall premature mortality burden decreases by 45.6~72.0 thousand instances (6.5%~10.3%) in Eastern China. Notably, the decline in premature deaths, especially those related to stroke, plays a significant role in the overall reduction.

6 Conclusions

Accurate NH_3 emission inventory is essential for developing effective air quality improvement policies. Numerous studies have demonstrated that the current bottom-up NH_3 emission inventories in China often underestimate the total NH_3 emissions, with significant uncertainties in the estimation of emissions from various sources. In this study, we used IASI satellite products and an iterative algorithm with the WRF-Chem model to optimize the bottom-up NH_3 emission inventory for Eastern China and further

https://doi.org/10.5194/egusphere-2025-1407
Preprint. Discussion started: 15 May 2025

assessed the impacts of NH_3 emission reductions from different sources on $PM_{2.5}$ concentrations

The results indicate that the NH_3 emission in Eastern China for 2016 amounted to 4.2 Tg. The highest emissions occurred in summer (463.1 Gg mon^{-1}), with AGR sources contributing 86.5% and non-AGR sources contributing 13.5%. In contrast, emissions were lowest in winter (217.4 Gg mon^{-1}), and the proportion of emissions from non-AGR sources were higher than that from AGR sources. Spatially, the region with the highest NH_3 emissions was located at the intersection of Henan, Hebei, and Shandong provinces. The optimization of the NH_3 inventory further improved the simulation underestimation of the NH_3 total column (MFB from -61% to -30%) and surface concentration (MFB from -61% to -19%). It also indirectly improved the simulation of other air pollutants, such as $PM_{2.5}$, NO_2 and SO_2.

Based on the posterior emission inventory, we conducted a series of sensitivity simulations to investigate the response of $PM_{2.5}$ concentrations to NH_3 emission reductions. A 30%~60% reduction in NH_3 emissions resulted in a 1.5~8.8 μg m^{-3} decrease in $PM_{2.5}$ concentrations. In terms of sectoral contributions, reductions in AGR emissions led to a decrease in $PM_{2.5}$ ranging from 0.9 μg m^{-3} to 7.4 μg m^{-3}, while the response to reductions in non-AGR NH_3 emissions ranged from 0.9 μg m^{-3} to 5.3 μg m^{-3}. Furthermore, the reduction in NH_3 emissions had a beneficial impact on public health, with a 6.5%~10.3% decrease in premature deaths attributed to $PM_{2.5}$ exposure.

This study obtained a high-resolution NH_3 emission inventory for Eastern China and highlights the significant role of non-AGR NH_3 emission reductions in further decreasing $PM_{2.5}$ levels. The findings provide robust data support for air quality research and offer scientific insights for exploring the potential air quality and public health benefits of NH_3 emission reduction.

Conflicts of Interest: The authors declare that the research was conducted in the absence of any commercial or financial relationships that could be construed as a potential conflict of interest.

Author Contributions: Data curation, model simulation, visualization, and writing-original draft preparation, KQT, HRZ, GX, FYC, JM, XC and YX; Supervision, funding acquisition, writing-review and editing, NL, HL, JBJ, BJL and KL. All authors have read and agreed to the published version of the manuscript.

Funding: This work was supported by the National Key Research and Development Program of China (2022YFC3701005), the special found of State Environmental Protection Key Laboratory of Formation and Prevention of Urban Air Pollution Complex (SEPAir-2024080216).

Acknowledgements: The numerical calculations in this paper have been done on the supercomputing system in the Supercomputing Center of Nanjing University of Information Science & Technology.

Reference

Bai L, Lu X, Yin S, Zhang H, Ma S, Wang C, et al. 2020. A recent emission inventory of multiple air pollutant, pm2.5 chemical species and its spatial-temporal characteristics in central china. Journal of Cleaner Production 269:122114.

Bessagnet, B., Beauchamp, M., Guerreiro, C., de Leeuw, F., Tsyro, S., Colette, A., Meleux, F., Rouïl, L., Ruyssenaars, P., Sauter, F., Velders, G. J. M., Foltescu, V. L., and van Aardenne, J.: Can further mitigation of ammonia emissions reduce exceedances of particulate matter air quality standards?, Environmental Science & Policy, 44, 149–163, https://doi.org/10.1016/j.envsci.2014.07.011, 2014.

Chang, Y., Deng, C., Dore, A. J., and Zhuang, G.: Human Excreta as a Stable and Important Source of Atmospheric Ammonia in the Megacity of Shanghai, PLoS One, 10, e0144661, https://doi.org/10.1371/journal.pone.0144661, 2015.

Chang, Y., Zou, Z., Deng, C., Huang, K., Collett, J. L., Lin, J., and Zhuang, G.: The importance of vehicle emissions as a source of atmospheric ammonia in the megacity of Shanghai, Atmospheric Chemistry and Physics, 16, 3577–3594, https://doi.org/10.5194/acp-16-3577-2016, 2016.

Chen, Y., Shen, H., Kaiser, J., Hu, Y., Capps, S. L., Zhao, S., Hakami, A., Shih, J.-S.,

https://doi.org/10.5194/egusphere-2025-1407
Preprint. Discussion started: 15 May 2025

Pavur, G. K., Turner, M. D., Henze, D. K., Resler, J., Nenes, A., Napelenok, S. L., Bash, J. O., Fahey, K. M., Carmichael, G. R., Chai, T., Clarisse, L., Coheur, P.-F., Van Damme, M., and Russell, A. G.: High-resolution hybrid inversion of IASI ammonia columns to constrain US ammonia emissions using the CMAQ adjoint model, Atmospheric Chemistry and Physics, 21, 2067–2082, https://doi.org/10.5194/acp-21-2067-2021, 2021.

Chen, Y., Zhang, Q., Cai, X., Zhang, H., Lin, H., Zheng, C., Guo, Z., Hu, S., Chen, L., Tao, S., Liu, M., and Wang, X.: Rapid Increase in China's Industrial Ammonia Emissions: Evidence from Unit-Based Mapping, Environ Sci Technol, https://doi.org/10.1021/acs.est.1c08369, 2022.

Cheng, L., Ye, Z., Cheng, S., and Guo, X.: Agricultural ammonia emissions and its impact on PM2.5 concentrations in the Beijing-Tianjin-Hebei region from 2000 to 2018, Environ Pollut, 291, 118162, https://doi.org/10.1016/j.envpol.2021.118162, 2021.

Du, P., Du, H., Zhang, W., Lu, K., Zhang, C., Ban, J., Wang, Y., Liu, T., Hu, J., and Li, T.: Unequal Health Risks and Attributable Mortality Burden of Source-Specific $PM_{2.5}$ in China, Environ. Sci. Technol., 58, 10897–10909, https://doi.org/10.1021/acs.est.3c08789, 2024.

Feng, S., Gao, D., Liao, F., Zhou, F., and Wang, X.: The health effects of ambient PM2.5 and potential mechanisms, Ecotoxicology and Environmental Safety, 128, 67–74, https://doi.org/10.1016/j.ecoenv.2016.01.030, 2016.

Feng, S., Xu, W., Cheng, M., Ma, Y., Wu, L., Kang, J., Wang, K., Tang, A., Collett, J. L., Fang, Y., Goulding, K., Liu, X., and Zhang, F.: Overlooked Nonagricultural and Wintertime Agricultural NH3 Emissions in Quzhou County, North China Plain: Evidence from 15N-Stable Isotopes, Environmental Science & Technology Letters, 9, 127–133, https://doi.org/10.1021/acs.estlett.1c00935, 2022.

Fu, X., Wang, S. X., Ran, L. M., Pleim, J. E., Cooter, E., Bash, J. O., Benson, V., and Hao, J. M.: Estimating NH₃ emissions from agricultural fertilizer application in China using the bi-directional CMAQ model coupled to an agro-ecosystem model, Atmos. Chem. Phys., 15, 6637–6649, https://doi.org/10.5194/acp-15-6637-2015, 2015.

Gao, D., Zhao, B., Wang, S., Wang, Y., Gaudet, B., Zhu, Y., Wang, X., Shen, J., Li, S., He, Y., Yin, D., and Dong, Z.: Increased importance of aerosol–cloud interactions for surface $PM_{2.5}$ pollution relative to aerosol–radiation interactions in China with the anthropogenic emission reductions, Atmos. Chem. Phys., 23, 14359–14373, https://doi.org/10.5194/acp-23-14359-2023, 2023.

Geng, G., Liu, Y., Liu, Y., Liu, S., Cheng, J., Yan, L., Wu, N., Hu, H., Tong, D., Zheng, B., Yin, Z., He, K., and Zhang, Q.: Efficacy of China's clean air actions to tackle

https://doi.org/10.5194/egusphere-2025-1407
Preprint. Discussion started: 15 May 2025

PM2.5 pollution between 2013 and 2020, Nat. Geosci., 17, 987–994, https://doi.org/10.1038/s41561-024-01540-z, 2024.

Guo, H., Otjes, R., Schlag, P., Kiendler-Scharr, A., Nenes, A., and Weber, R. J.: Effectiveness of ammonia reduction on control of fine particle nitrate, Atmospheric Chemistry and Physics, 18, 12241–12256, https://doi.org/10.5194/acp-18-12241-2018, 2018.

Guo, X., Ye, Z., Chen, D., Wu, H., Shen, Y., Liu, J., and Cheng, S.: Prediction and mitigation potential of anthropogenic ammonia emissions within the Beijing-Tianjin-Hebei region, China, Environ Pollut, 259, 113863, https://doi.org/10.1016/j.envpol.2019.113863, 2020.

Guo, Y., Zhang, L., Winiwarter, W., Van Grinsven, H. J. M., Wang, X., Li, K., Pan, D., Liu, Z., and Gu, B.: Ambitious nitrogen abatement is required to mitigate future global PM2.5 air pollution toward the World Health Organization targets, One Earth, 7, 1600–1613, https://doi.org/10.1016/j.oneear.2024.08.007, 2024.

Hu, S., Zhao, G., Tan, T., Li, C., Zong, T., Xu, N., Zhu, W., and Hu, M.: Current challenges of improving visibility due to increasing nitrate fraction in PM2.5 during the haze days in Beijing, China, Environmental Pollution, 290, 118032, https://doi.org/10.1016/j.envpol.2021.118032, 2021.

Huang, L., Zhu, Y., Zhai, H., Xue, S., Zhu, T., Shao, Y., Liu, Z., Emery, C., Yarwood, G., Wang, Y., Fu, J., Zhang, K., and Li, L.: Recommendations on benchmarks for numerical air quality model applications in China – Part 1: $PM_{2.5}$ and chemical species, Atmos. Chem. Phys., 21, 2725–2743, https://doi.org/10.5194/acp-21-2725-2021, 2021.

Huang, R.-J., Zhang, Y., Bozzetti, C., Ho, K.-F., Cao, J.-J., Han, Y., Daellenbach, K. R., Slowik, J. G., Platt, S. M., Canonaco, F., Zotter, P., Wolf, R., Pieber, S. M., Bruns, E. A., Crippa, M., Ciarelli, G., Piazzalunga, A., Schwikowski, M., Abbaszade, G., Schnelle-Kreis, J., Zimmermann, R., An, Z., Szidat, S., Baltensperger, U., Haddad, I. E., and Prévôt, A. S. H.: High secondary aerosol contribution to particulate pollution during haze events in China, Nature, 514, 218–222, https://doi.org/10.1038/nature13774, 2014.

Huang, X., Song, Y., Li, M., Li, J., Huo, Q., Cai, X., Zhu, T., Hu, M., and Zhang, H.: A high-resolution ammonia emission inventory in China, Global Biogeochemical Cycles, 26, n/a-n/a, https://doi.org/10.1029/2011gb004161, 2012.

Kang, Y., Liu, M., Song, Y., Huang, X., Yao, H., Cai, X., Zhang, H., Kang, L., Liu, X., Yan, X., He, H., Zhang, Q., Shao, M., and Zhu, T.: High-resolution ammonia emissions inventories in China from 1980 to 2012, Atmospheric Chemistry and Physics, 16, 2043–2058, https://doi.org/10.5194/acp-16-2043-2016, 2016.

https://doi.org/10.5194/egusphere-2025-1407
Preprint. Discussion started: 15 May 2025

Kong, L., Tang, X., Zhu, J., Wang, Z., Pan, Y., Wu, H., Wu, L., Wu, Q., He, Y., Tian, S., Xie, Y., Liu, Z., Sui, W., Han, L., and Carmichael, G.: Improved Inversion of Monthly Ammonia Emissions in China Based on the Chinese Ammonia Monitoring Network and Ensemble Kalman Filter, Environ Sci Technol, 53, 12529–12538, https://doi.org/10.1021/acs.est.9b02701, 2019.

Lei, R., Nie, D., Zhang, S., Yu, W., Ge, X., and Song, N.: Spatial and temporal characteristics of air pollutants and their health effects in China during 2019–2020, Journal of Environmental Management, 317, 115460, https://doi.org/10.1016/j.jenvman.2022.115460, 2022.

Lei, Y., Yin, Z., Lu, X., Zhang, Q., Gong, J., Cai, B., Cai, C., Chai, Q., Chen, H., Chen, R., Chen, S., Chen, W., Cheng, J., Chi, X., Dai, H., Feng, X., Geng, G., Hu, J., Hu, S., Huang, C., Li, T., Li, W., Li, X., Liu, J., Liu, X., Liu, Z., Ma, J., Qin, Y., Tong, D., Wang, X., Wang, X., Wu, R., Xiao, Q., Xie, Y., Xu, X., Xue, T., Yu, H., Zhang, D., Zhang, N., Zhang, S., Zhang, S., Zhang, X., Zhang, X., Zhang, Z., Zheng, B., Zheng, Y., Zhou, J., Zhu, T., Wang, J., and He, K.: The 2022 report of synergetic roadmap on carbon neutrality and clean air for China: Accelerating transition in key sectors, Environmental Science and Ecotechnology, 19, 100335, https://doi.org/10.1016/j.ese.2023.100335, 2024.

Li, B., Chen, L., Shen, W., Jin, J., Wang, T., Wang, P., Yang, Y., and Liao, H.: Improved gridded ammonia emission inventory in China, Atmospheric Chemistry and Physics, 21, 15883–15900, https://doi.org/10.5194/acp-21-15883-2021, 2021.

Li, B., Liao, H., Li, K., Wang, Y., Zhang, L., Guo, Y., Liu, L., Li, J., Jin, J., Yang, Y., Gong, C., Wang, T., Shen, W., Wang, P., Dang, R., Liao, K., Zhu, Q., and Jacob, D. J.: Unlocking nitrogen management potential via large-scale farming for air quality and substantial co-benefits, National Science Review, 11, nwae324, https://doi.org/10.1093/nsr/nwae324, 2024.

Li, M., Liu, H., Geng, G., Hong, C., Liu, F., Song, Y., Tong, D., Zheng, B., Cui, H., Man, H., Zhang, Q., and He, K.: Anthropogenic emission inventories in China: a review, National Science Review, 4, 834–866, https://doi.org/10.1093/nsr/nwx150, 2017.

Li, N., Zhang, H., Zhu, S., Liao, H., Hu, J., Tang, K., Feng, W., Zhang, R., Shi, C., Xu, H., Chen, L., and Li, J.: Secondary PM2.5 dominates aerosol pollution in the Yangtze River Delta region: Environmental and health effects of the Clean air Plan, Environment International, 171, 107725, https://doi.org/10.1016/j.envint.2022.107725, 2023a.

Li, R., Gao, Y., Xu, J., Cui, L., and Wang, G.: Impact of Clean Air Policy on Criteria Air Pollutants and Health Risks Across China During 2013–2021, JGR Atmospheres, 128, e2023JD038939, https://doi.org/10.1029/2023JD038939, 2023b.

Liu, H., Lei, J., Liu, Y., Zhu, T., Chan, K., Chen, X., Wei, J., Deng, F., Li, G., Jiang, Y., Bai, L., Wang, K., Chen, J., Lan, Y., Xia, X., Wang, J., Wei, C., Li, Y., Chen, R., Gong, J., Duan, X., Zhang, K., Kan, H., Shi, X., Guo, X., and Wu, S.: Hospital admissions attributable to reduced air pollution due to clean-air policies in China, Nat Med, https://doi.org/10.1038/s41591-025-03515-y, 2025.

Liu, M., Huang, X., Song, Y., Tang, J., Cao, J., Zhang, X., Zhang, Q., Wang, S., Xu, T., Kang, L., Cai, X., Zhang, H., Yang, F., Wang, H., Yu, J. Z., Lau, A. K. H., He, L., Huang, X., Duan, L., Ding, A., Xue, L., Gao, J., Liu, B., and Zhu, T.: Ammonia emission control in China would mitigate haze pollution and nitrogen deposition, but worsen acid rain, Proc Natl Acad Sci U S A, 116, 7760–7765, https://doi.org/10.1073/pnas.1814880116, 2019.

Liu, P., Ding, J., Liu, L., Xu, W., and Liu, X.: Estimation of surface ammonia concentrations and emissions in China from the polar-orbiting Infrared Atmospheric Sounding Interferometer and the FY-4A Geostationary Interferometric Infrared Sounder, Atmos. Chem. Phys., 22, 9099–9110, https://doi.org/10.5194/acp-22-9099-2022, 2022a.

Liu, R., Liu, T., Huang, X., Ren, C., Wang, L., Niu, G., Yu, C., Zhang, Y., Wang, J., Qi, X., Nie, W., Chi, X., and Ding, A.: Characteristics and sources of atmospheric ammonia at the SORPES station in the western Yangtze river delta of China, Atmospheric Environment, 318, 120234, https://doi.org/10.1016/j.atmosenv.2023.120234, 2024.

Liu, S., Geng, G., Xiao, Q., Zheng, Y., Liu, X., Cheng, J., and Zhang, Q.: Tracking Daily Concentrations of PM2.5 Chemical Composition in China since 2000, Environ. Sci. Technol., 56, 16517–16527, https://doi.org/10.1021/acs.est.2c06510, 2022b.

Liu, Z., Zhou, M., Chen, Y., Chen, D., Pan, Y., Song, T., Ji, D., Chen, Q., and Zhang, L.: The nonlinear response of fine particulate matter pollution to ammonia emission reductions in North China, Environmental Research Letters, https://doi.org/10.1088/1748-9326/abdf86, 2021.

Liu, Z., Rieder, H. E., Schmidt, C., Mayer, M., Guo, Y., Winiwarter, W., and Zhang, L.: Optimal reactive nitrogen control pathways identified for cost-effective PM2.5 mitigation in Europe, Nat Commun, 14, 4246, https://doi.org/10.1038/s41467-023-39900-9, 2023.

Lu, L., Yuan, L., Cai, Z., Fu, J., and Wu, G.: Emission inventory and distribution characteristics of NH3 from agricultural fertilizers in Hunan, China, from 2012 to 2021, Atmospheric Pollution Research, 16, 102479, https://doi.org/10.1016/j.apr.2025.102479, 2025.

Ma, S.: High-resolution assessment of ammonia emissions in China: Inventories, driving forces and mitigation, Atmospheric Environment, 229, 117458, https://doi.org/10.1016/j.atmosenv.2020.117458, 2020.

Pan, D., Mauzerall, D. L., Wang, R., Guo, X., Puchalski, M., Guo, Y., Song, S., Tong, D., Sullivan, A. P., Schichtel, B. A., Collett, J. L., and Zondlo, M. A.: Regime shift in secondary inorganic aerosol formation and nitrogen deposition in the rural United States, Nat. Geosci., 17, 617–623, https://doi.org/10.1038/s41561-024-01455-9, 2024.

Pan, Y., Tian, S., Liu, D., Fang, Y., Zhu, X., Zhang, Q., Zheng, B., Michalski, G., and Wang, Y.: Fossil Fuel Combustion-Related Emissions Dominate Atmospheric Ammonia Sources during Severe Haze Episodes: Evidence from (15)N-Stable Isotope in Size-Resolved Aerosol Ammonium, Environ Sci Technol, 50, 8049–56, https://doi.org/10.1021/acs.est.6b00634, 2016.

Pan, Y., Tian, S., Zhao, Y., Zhang, L., Zhu, X., Gao, J., Huang, W., Zhou, Y., Song, Y., Zhang, Q., and Wang, Y.: Identifying Ammonia Hotspots in China Using a National Observation Network, Environ Sci Technol, 52, 3926–3934, https://doi.org/10.1021/acs.est.7b05235, 2018a.

Pan, Y., Tian, S., Liu, D., Fang, Y., Zhu, X., Gao, M., Gao, J., Michalski, G., and Wang, Y.: Isotopic evidence for enhanced fossil fuel sources of aerosol ammonium in the urban atmosphere, Environ Pollut, 238, 942–947, https://doi.org/10.1016/j.envpol.2018.03.038, 2018b.

Paulot, F., Jacob, D. J., Pinder, R. W., Bash, J. O., Travis, K., and Henze, D. K.: Ammonia emissions in the United States, European Union, and China derived by high-resolution inversion of ammonium wet deposition data: Interpretation with a new agricultural emissions inventory (MASAGE_NH3), Journal of Geophysical Research: Atmospheres, 119, 4343–4364, https://doi.org/10.1002/2013jd021130, 2014.

Pendergrass, D. C., Jacob, D. J., Oak, Y. J., Lee, J., Kim, M., Kim, J., Lee, S., Zhai, S., Irie, H., and Liao, H.: A continuous 2011–2022 record of fine particulate matter (PM2.5) in East Asia at daily 2-km resolution from geostationary satellite observations: Population exposure and long-term trends, Atmospheric Environment, 346, 121068, https://doi.org/10.1016/j.atmosenv.2025.121068, 2025.

Peng, Z., Wang, H., Zhang, M., Zhang, Y., Li, L., Li, Y., and Ao, Z.: Analysis of aerosol chemical components and source apportionment during a long-lasting haze event in the Yangtze River Delta, China, Journal of Environmental Sciences, 156, 14–29, https://doi.org/10.1016/j.jes.2024.06.023, 2025.

Pu, W., Ma, Z., Collett, J. L., Guo, H., Lin, W., Cheng, Y., Quan, W., Li, Y., Dong, F., and He, D.: Regional transport and urban emissions are important ammonia

https://doi.org/10.5194/egusphere-2025-1407
Preprint. Discussion started: 15 May 2025

contributors in Beijing, China, Environ Pollut, 265, 115062, https://doi.org/10.1016/j.envpol.2020.115062, 2020.

Ren, C., Huang, X., Liu, T., Song, Y., Wen, Z., Liu, X., Ding, A., and Zhu, T.: A dynamic ammonia emission model and the online coupling with WRF–Chem (WRF–SoilN–Chem v1.0): development and regional evaluation in China, Geoscientific Model Development, 16, 1641–1659, https://doi.org/10.5194/gmd-16-1641-2023, 2023.

Ren, C., Huang, X., Wang, Y., Zhang, L., Zhou, X., Sun, W., Zhang, H., Liu, T., Ding, A., and Wang, T.: Enhanced Soil Emissions of Reactive Nitrogen Gases by Fertilization and Their Impacts on Secondary Air Pollution in Eastern China, Environ. Sci. Technol., 59, 5119–5130, https://doi.org/10.1021/acs.est.4c12324, 2025.

Song, L., Walters, W. W., Pan, Y., Li, Z., Gu, M., Duan, Y., Lü, X., and Fang, Y.: 15N natural abundance of vehicular exhaust ammonia, quantified by active sampling techniques, Atmospheric Environment, 255, 118430, https://doi.org/10.1016/j.atmosenv.2021.118430, 2021.

Song, Q., Huang, L., Zhang, Y., Li, Z., Wang, S., Zhao, B., Yin, D., Ma, M., Li, S., Liu, B., Zhu, L., Chang, X., Gao, D., Jiang, Y., Dong, Z., Shi, H., and Hao, J.: Driving Factors of $PM_{2.5}$ Pollution Rebound in North China Plain in Early 2023, Environ. Sci. Technol. Lett., 12, 305–312, https://doi.org/10.1021/acs.estlett.4c01153, 2025.

Sun, K., Tao, L., Miller, D. J., Pan, D., Golston, L. M., Zondlo, M. A., Griffin, R. J., Wallace, H. W., Leong, Y. J., Yang, M. M., Zhang, Y., Mauzerall, D. L., and Zhu, T.: Vehicle Emissions as an Important Urban Ammonia Source in the United States and China, Environ Sci Technol, 51, 2472–2481, https://doi.org/10.1021/acs.est.6b02805, 2017.

Ti, C., Han, X., Chang, S. X., Peng, L., Xia, L., and Yan, X.: Mitigation of agricultural NH3 emissions reduces PM2.5 pollution in China: A finer scale analysis, Journal of Cleaner Production, 350, 131507, https://doi.org/10.1016/j.jclepro.2022.131507, 2022.

Van Damme, M., Whitburn, S., Clarisse, L., Clerbaux, C., Hurtmans, D., and Coheur, P.-F.: Version 2 of the IASI NH₃ neural network retrieval algorithm: near-real-time and reanalysed datasets, Atmospheric Measurement Techniques, 10, 4905–4914, https://doi.org/10.5194/amt-10-4905-2017, 2017.

Van Damme, M., Clarisse, L., Whitburn, S., Hadji-Lazaro, J., Hurtmans, D., Clerbaux, C., and Coheur, P. F.: Industrial and agricultural ammonia point sources exposed, Nature, 564, 99–103, https://doi.org/10.1038/s41586-018-0747-1, 2018.

Wang, G., Zhang, R., Gomez, M. E., Yang, L., Levy Zamora, M., Hu, M., Lin, Y., Peng, J., Guo, S., Meng, J., Li, J., Cheng, C., Hu, T., Ren, Y., Wang, Y., Gao, J., Cao, J., An, Z., Zhou, W., Li, G., Wang, J., Tian, P., Marrero-Ortiz, W., Secrest, J., Du, Z., Zheng, J., Shang, D., Zeng, L., Shao, M., Wang, W., Huang, Y., Wang, Y., Zhu, Y., Li, Y., Hu, J., Pan, B., Cai, L., Cheng, Y., Ji, Y., Zhang, F., Rosenfeld, D., Liss, P. S., Duce, R. A., Kolb, C. E., and Molina, M. J.: Persistent sulfate formation from London Fog to Chinese haze, Proc Natl Acad Sci U S A, 113, 13630–13635, https://doi.org/10.1073/pnas.1616540113, 2016.

Wang, J., Zhao, B., Wang, S., Yang, F., Xing, J., Morawska, L., Ding, A., Kulmala, M., Kerminen, V.-M., Kujansuu, J., Wang, Z., Ding, D., Zhang, X., Wang, H., Tian, M., Petäjä, T., Jiang, J., and Hao, J.: Particulate matter pollution over China and the effects of control policies, Science of The Total Environment, 584–585, 426–447, https://doi.org/10.1016/j.scitotenv.2017.01.027, 2017.

Wei, J., Li, Z., Chen, X., Li, C., Sun, Y., Wang, J., Lyapustin, A., Brasseur, G. P., Jiang, M., Sun, L., Wang, T., Jung, C. H., Qiu, B., Fang, C., Liu, X., Hao, J., Wang, Y., Zhan, M., Song, X., and Liu, Y.: Separating Daily 1 km PM2.5 Inorganic Chemical Composition in China since 2000 via Deep Learning Integrating Ground, Satellite, and Model Data, Environ. Sci. Technol., 57, 18282–18295, https://doi.org/10.1021/acs.est.3c00272, 2023.

Wu, C., Wang, G., Li, J., Li, J., Cao, C., Ge, S., Xie, Y., Chen, J., Liu, S., Du, W., Zhao, Z., and Cao, F.: Non-agricultural sources dominate the atmospheric NH3 in Xi'an, a megacity in the semi-arid region of China, Sci Total Environ, 722, 137756, https://doi.org/10.1016/j.scitotenv.2020.137756, 2020.

Xiao, Q., Geng, G., Xue, T., Liu, S., Cai, C., He, K., and Zhang, Q.: Tracking $PM_{2.5}$ and O_3 Pollution and the Related Health Burden in China 2013–2020, Environ. Sci. Technol., 56, 6922–6932, https://doi.org/10.1021/acs.est.1c04548, 2022.

Xu, W., Zhao, Y., Wen, Z., Chang, Y., Pan, Y., Sun, Y., Ma, X., Sha, Z., Li, Z., Kang, J., Liu, L., Tang, A., Wang, K., Zhang, Y., Guo, Y., Zhang, L., Sheng, L., Zhang, X., Gu, B., Song, Y., Van Damme, M., Clarisse, L., Coheur, P.-F., Collett, J. L., Goulding, K., Zhang, F., He, K., and Liu, X.: Increasing importance of ammonia emission abatement in PM2.5 pollution control, Science Bulletin, 67, 1745–1749, https://doi.org/10.1016/j.scib.2022.07.021, 2022.

Yang, G., Ren, G., Zhang, P., Xue, X., Tysa, S. K., Jia, W., Qin, Y., Zheng, X., and Zhang, S.: $PM_{2.5}$ Influence on Urban Heat Island (UHI) Effect in Beijing and the Possible Mechanisms, JGR Atmospheres, 126, e2021JD035227, https://doi.org/10.1029/2021JD035227, 2021.

Yang, Z., Wang, Y., Xu, X.-H., Yang, J., and Ou, C.-Q.: Quantifying and characterizing the impacts of PM2.5 and humidity on atmospheric visibility in 182 Chinese cities: A nationwide time-series study, Journal of Cleaner Production, 368, 133182, https://doi.org/10.1016/j.jclepro.2022.133182, 2022.

https://doi.org/10.5194/egusphere-2025-1407
Preprint. Discussion started: 15 May 2025

Zhang, H., Zhou, X., Ren, C., Li, M., Liu, T., and Huang, X.: A systematic review of reactive nitrogen simulations with chemical transport models in China, Atmospheric Research, 309, 107586, https://doi.org/10.1016/j.atmosres.2024.107586, 2024.

Zhang, L., Chen, Y., Zhao, Y., Henze, D. K., Zhu, L., Song, Y., Paulot, F., Liu, X., Pan, Y., Lin, Y., and Huang, B.: Agricultural ammonia emissions in China: reconciling bottom-up and top-down estimates, Atmospheric Chemistry and Physics, 18, 339–355, https://doi.org/10.5194/acp-18-339-2018, 2018.

Zhang, Q., Zheng, Y., Tong, D., Shao, M., Wang, S., Zhang, Y., Xu, X., Wang, J., He, H., Liu, W., Ding, Y., Lei, Y., Li, J., Wang, Z., Zhang, X., Wang, Y., Cheng, J., Liu, Y., Shi, Q., Yan, L., Geng, G., Hong, C., Li, M., Liu, F., Zheng, B., Cao, J., Ding, A., Gao, J., Fu, Q., Huo, J., Liu, B., Liu, Z., Yang, F., He, K., and Hao, J.: Drivers of improved PM2.5 air quality in China from 2013 to 2017, Proc Natl Acad Sci U S A, 116, 24463–24469, https://doi.org/10.1073/pnas.1907956116, 2019.

Zhang, X., Wu, Y., Liu, X., Reis, S., Jin, J., Dragosits, U., Van Damme, M., Clarisse, L., Whitburn, S., Coheur, P. F., and Gu, B.: Ammonia Emissions May Be Substantially Underestimated in China, Environ Sci Technol, 51, 12089–12096, https://doi.org/10.1021/acs.est.7b02171, 2017.

Zhang, Z., Yan, Y., Kong, S., Deng, Q., Qin, S., Yao, L., Zhao, T., and Qi, S.: Benefits of refined NH3 emission controls on PM2.5 mitigation in Central China, Sci Total Environ, 814, 151957, https://doi.org/10.1016/j.scitotenv.2021.151957, 2022.

Zhao, Y., Yuan, M., Huang, X., Chen, F., and Zhang, J.: Quantification and evaluation of atmospheric ammonia emissions with different methods: a case study for the Yangtze River Delta region, China, Atmospheric Chemistry and Physics, 20, 4275–4294, https://doi.org/10.5194/acp-20-4275-2020, 2020.

Zheng, B., Zhang, Q., Zhang, Y., He, K. B., Wang, K., Zheng, G. J., Duan, F. K., Ma, Y. L., and Kimoto, T.: Heterogeneous chemistry: a mechanism missing in current models to explain secondary inorganic aerosol formation during the January 2013 haze episode in North China, Atmospheric Chemistry and Physics, 15, 2031–2049, https://doi.org/10.5194/acp-15-2031-2015, 2015.

Zheng, B., Tong, D., Li, M., Liu, F., Hong, C., Geng, G., Li, H., Li, X., Peng, L., Qi, J., Yan, L., Zhang, Y., Zhao, H., Zheng, Y., He, K., and Zhang, Q.: Trends in China's anthropogenic emissions since 2010 as the consequence of clean air actions, Atmospheric Chemistry and Physics, 18, 14095–14111, https://doi.org/10.5194/acp-18-14095-2018, 2018.

Zhou, M., Jiang, W., Gao, W., Gao, X., Ma, M., and Ma, X.: Anthropogenic emission inventory of multiple air pollutants and their spatiotemporal variations in 2017 for the Shandong Province, China, Environ Pollut, 288, 117666, https://doi.org/10.1016/j.envpol.2021.117666, 2021.

Zhou, M., Nie, W., Qiao, L., Huang, D. D., Zhu, S., Lou, S., Wang, H., Wang, Q., Tao, S., Sun, P., Liu, Y., Xu, Z., An, J., Yan, R., Su, H., Huang, C., Ding, A., and Chen, C.: Elevated Formation of Particulate Nitrate From N_2O_5 Hydrolysis in the Yangtze River Delta Region From 2011 to 2019, Geophysical Research Letters, 49, e2021GL097393, https://doi.org/10.1029/2021GL097393, 2022.

Zhu, Q., Deng, Y.-L., Liu, Y., and Steenland, K.: Associations between Ultrafine Particles and Incident Dementia in Older Adults, Environ. Sci. Technol., acs.est.4c10574, https://doi.org/10.1021/acs.est.4c10574, 2025.

https://doi.org/10.5194/egusphere-2025-1407
Preprint. Discussion started: 15 May 2025

Table 1. NH_3 emission estimates in recent studies

Region	Sector	Emission	Period	Method	Reference
China	/	12.4 Tg yr^{-1}	2016	Bottom-up	Ma (2020)
		12.1 Tg yr^{-1}	2016	Bottom-up	Li et al. (2021)
		11.9~12.0 Tg yr^{-1}	2005~2015	Bottom-up	Chen et al. (2021)
		11.7 Tg yr^{-1}	2008	Top-down	Zhang et al. (2018)
		8.4 Tg N yr^{-1}	2005-2008	Top-down	Paulot et al. (2014)
		0.74 Tg mon^{-1}	2008 Apr	Top-down	Xu et al. (2013)
		13.0 Tg yr^{-1}	2016	Top-down	Kong et al. (2019)
		18.9 Tg yr^{-1}	2015	Top-down	Zhang et al. (2017)
Eastern China	Industry	274.5 Gg yr^{-1}	2016	Bottom-up	Chen et al. (2022)
BTH	/	966.1 Gg yr^{-1}	2016	Bottom-up	(Guo et al., 2020)
	/	28.8 Gg mon^{-1}	2015 Jan	Top-down	Huang et al. (2021)
		82.5 Gg mon^{-1}	2015 Apr		
		102.9 Gg mon^{-1}	2015 Jul		
		50.2 Gg mon^{-1}	2015 Oct		
	Agriculture	505.85 Gg yr^{-1}	2016	Top-down	This study
	Non-Agriculture	282.53 Gg yr^{-1}			
YRD	Agriculture	848.8 Gg yr^{-1}	2014	Bottom-up	Yu et al. (2020)
	Non-	137.2 Gg yr^{-1}			

https://doi.org/10.5194/egusphere-2025-1407
Preprint. Discussion started: 15 May 2025

	Agriculture				
	Agriculture	77 Gg mon^{-1}	2014 Jan	Bottom-up	Zhao et al. (2020)
		133 Gg mon^{-1}	2014 Apr		
		169 Gg mon^{-1}	2014 Jul		
		108 Gg mon^{-1}	2014 Oct		
	/	24.42 Gg mon^{-1}	2015 Jan	Top-down	Huang et al. (2021)
		88.0 Gg mon^{-1}	2015 Apr		
		111.7 Gg mon^{-1}	2015 Jul		
		51.0 Gg mon^{-1}	2015 Oct		
	Agriculture	1280.41 Gg	2016	Top-down	this study
	Non-Agriculture	297.86 Gg			
Henan	/	1035Gg yr^{-1}	2013	Top-down	Wang et al. (2018)
		982 Gg yr^{-1}	2016	Bottom-up	Bai et al. (2020)
	Agriculture	647.73 Gg yr^{-1}	2016	Top-down	this study
	Non-Agriculture	206.20 Gg yr^{-1}			
Shandong	/	1210 Gg yr^{-1}	2017	Bottom-up	Zhou et al. (2021)
	Agriculture	715.29 Gg yr^{-1}	2016	Top-down	this study
	Non-Agriculture	296.98 Gg yr^{-1}			

https://doi.org/10.5194/egusphere-2025-1407
Preprint. Discussion started: 15 May 2025

Table 2 List of sensitivity tests for optimized iterative algorithm.

Case name	AGR emission	Non-AGR emission	Emission outside the domain
A_{total}	√	√	√
A_{agr}	√	×	×
$A_{non\text{-}agr}$	×	√	×
$A_{transport}$	×	×	√
A_{blank}	×	×	×

https://doi.org/10.5194/egusphere-2025-1407
Preprint. Discussion started: 15 May 2025

Table 3 Simulated and observed air pollutant concentrations

	Prior simulation	Posterior simulation	Observation
$PM_{2.5}$ (μg m^{-3})	65.7	67.3	67.1
NO_2 (ppb)	22.3	22.1	23.0
SO_2 (ppb)	8.2	6.8	6.5

https://doi.org/10.5194/egusphere-2025-1407
Preprint. Discussion started: 15 May 2025

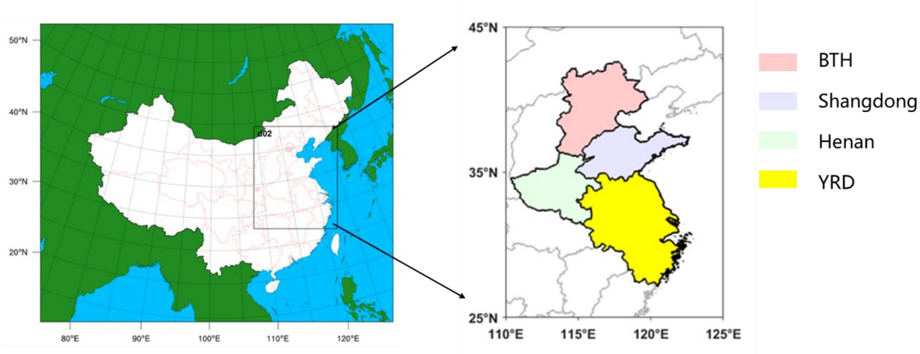

Figure 1. Simulation domains of the WRF-Chem model used in this study (left). Right panel illustrates the four research regions in Eastern China. Names and locations are labeled with different colors in this panel.

https://doi.org/10.5194/egusphere-2025-1407
Preprint. Discussion started: 15 May 2025

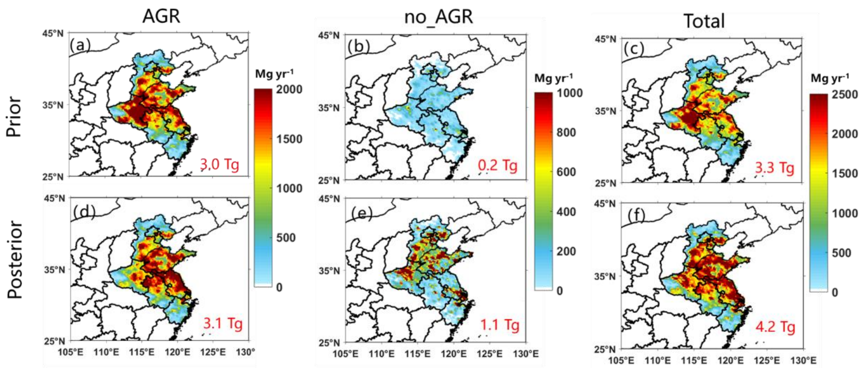

Figure 2. Prior and posterior NH_3 emissions from agricultural and non-agricultural sectors in the study region. The red numbers show the total emissions.

https://doi.org/10.5194/egusphere-2025-1407
Preprint. Discussion started: 15 May 2025

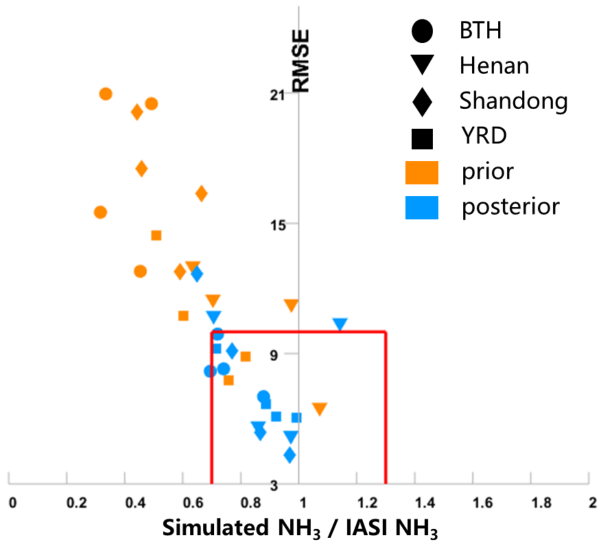

Figure 3. Scatter plots of the prior and posterior NH_3 total column data versus IASI retrievals. Each point represents prior (or posterior) data for a specific season and a specific region. Circles, triangles, rhombuses, and rectangles correspond to the BTH, Henan, Shandong, and YRD regions, respectively. Orange and blue markers represent a prior and a posterior data, respectively.

https://doi.org/10.5194/egusphere-2025-1407
Preprint. Discussion started: 15 May 2025

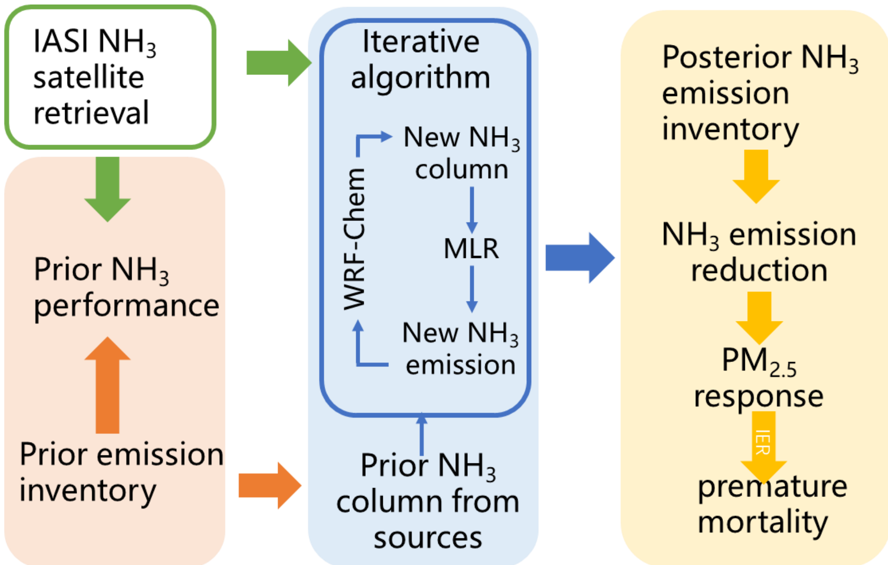

Figure 4. Visualization of the workflow in this study.

https://doi.org/10.5194/egusphere-2025-1407
Preprint. Discussion started: 15 May 2025

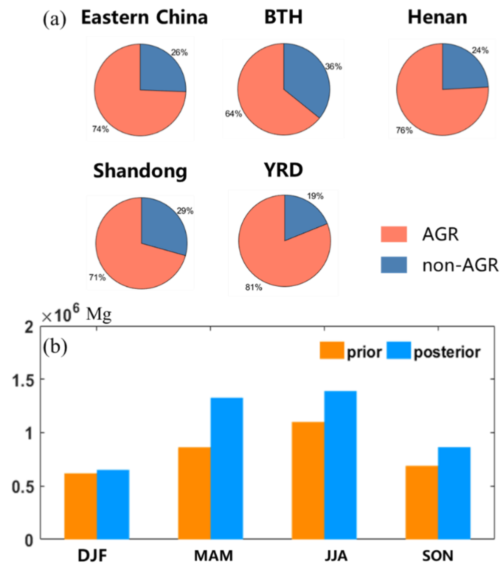

Figure 5. Posterior emission characteristics. (a) Contribution from regional emission sectors. (b) Comparison of the posteriori and prior emissions (unit: Mg) in study region.

https://doi.org/10.5194/egusphere-2025-1407
Preprint. Discussion started: 15 May 2025

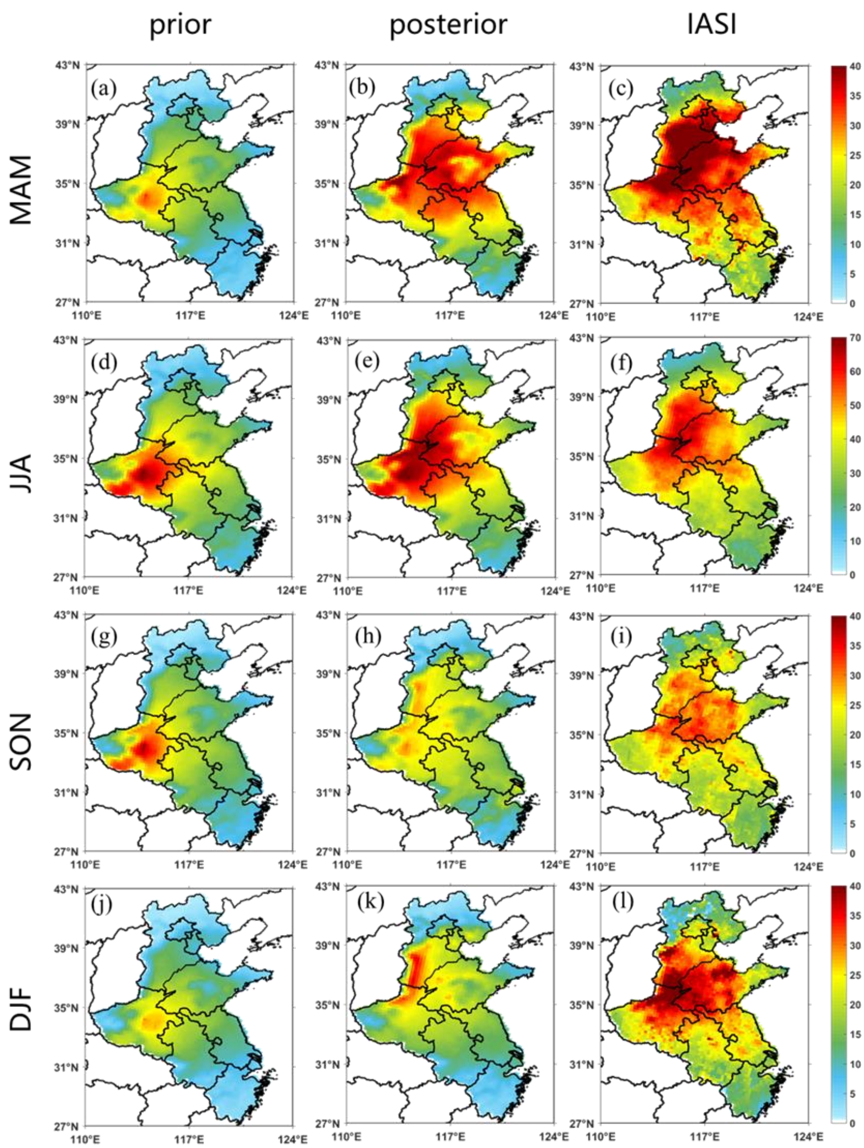

Figure 6. Distributions of NH_3 total column from prior simulation, posterior simulation and satellite retrieval in different seasons.

https://doi.org/10.5194/egusphere-2025-1407
Preprint. Discussion started: 15 May 2025

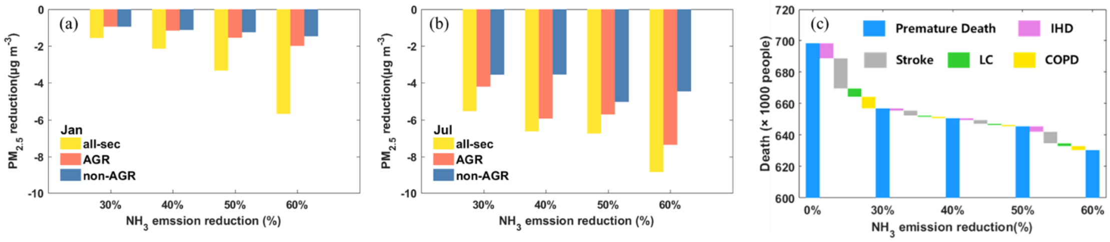

Figure 7. Response of NH_3 emission reduction in 30-60% in (a)-(b) concentration of $PM_{2.5}$ and (c) premature death caused by different diseases. The IHD, Stroke, LC and COPD represent the premature death caused by ischemic heart disease, stroke, lung cancer, chronic obstructive pulmonary disease.